CHAPTER II
LITERATURE REVIEW

2.1 Papers

2.1.1 Layered Structure of Paper

Paper is a layered sheet of interlocking cellulosic fibers held together by hydrogen bonds (Robert, 1996). It is formed continuously by a pulsed filtration process from an aqueous suspension of cellulosic fibers with possible addition of some polymeric retention aids and inorganic fillers. The cellulosic fibers are highly hydrophilic and are readily wetted and swollen by water. During the sheet forming process, as water is evaporated, the wet fibers are drawn close by the surface-tension force and ultimately held together by hydrogen bonds between the hydroxyl groups in the opposing fiber surfaces

2.2 Plant Fibers

2.2.1 Different Types of Plant Fibers

Fibers obtained from the various parts of the plants are known as plant fibers. Plant fibers include bast, leaf and seed/fruit fibers. Bast consists of a wood core surrounded by a stem. Within the stem, there are a number of fiber bundles, each containing individual fiber cells or filaments. Examples include flax, hemp, jute, kenaf and ramie. Leaf fibers such as sisal, abaca, banana and henequen are coarser than bast fibers. Cotton is the most common seed fiber. Other examples include coir and oil palm. Other source of lignocellulosics can be from agricultural residues such as rice hulls from a rice processing plant, sun flower seed hulls from an oil processing unit and bagasse from a sugar mill. The properties of natural fibers vary considerably depending on the fiber diameter, structure, degree of polymerization, crystal structure and source, whether the fibers are taken from the plant stem, leaf or seed, and on the growing conditions (Bledski and Gassan, 1999; Mohanty *et al.*, 2005; Nevell and Zeronian, 1985).

2.2.2 General Structure of Plant Fibers

A single or elementary plant fiber is a single cell typically of a length from 1 to 50 mm and a diameter of around 10–50 mm. Plant fibers are like microscopic tubes, for example, cell walls surrounding the central lumen. The lumen contributes to the water uptake behavior of plant fibers (Toumis, 1991). The fiber consists of several cell walls. These cell walls are formed from oriented reinforcing semi-crystalline cellulose micro fibrils embedded in a hemicellulose–lignin matrix of varying composition. Such microfibrils have typically a diameter of about 10–30 nm and are made up of 30–100 cellulose molecules in extended chain conformation and provide mechanical strength to the fiber. Figure 2.1 shows the arrangement of fibrils, microfibrils and cellulose in the cell walls of a plant fiber.

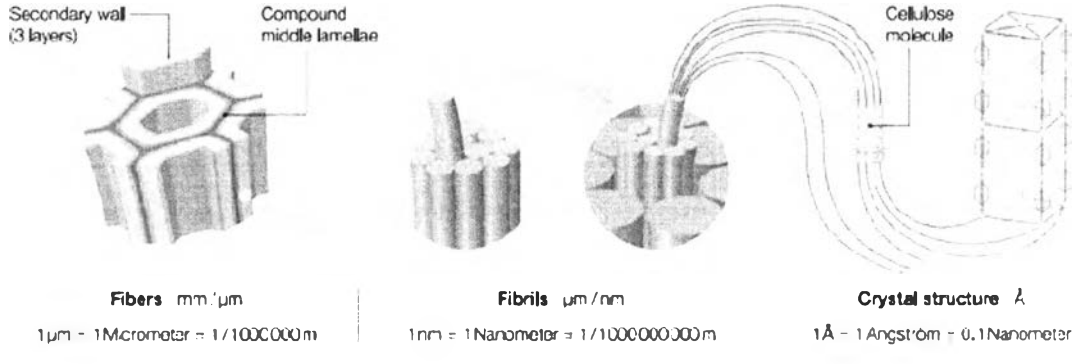

Figure 2.1 Arrangement of microfibrils and cellulose in the plant cell wall (Zimmermann *et al.*, 2004).

The hemicellulose molecules of the matrix phase in a cell wall are hydrogen bonded to cellulose and act as a cementing matrix between the cellulose microfibrils, forming the cellulose/hemicellulose network, which is thought to be the main structural component of the fiber cell. The hydrophobic lignins on the other hand act as a cementing agent and increase the stiffness of the cellulose/hemicellulose composite.

The cell walls are divided into two sections, the primary cell wall containing a loose irregular network of cellulose microfibrils, which are closely packed, and the secondary wall. The secondary wall is composed of three separate

and distant layers – S1 (outer layer), S2 (middle layer) and S3 (inner layer). S2 layer is the thickest and the most important in determining mechanical properties (Toumis, 1991). Schematic representation of the fine structure of a lignocellulosic fiber is presented in Figure 2.2 These fibre cell walls differ in their composition, i.e., the ratio between cellulose and lignin/hemicellulose and in the orientation or spiral angle of the cellulose microfibrils (Rong *et al.*, 2001). The spiral angle is the angle that the helical spirals of cellulose microfibrils form with the fiber axis. The spiral angle or the microfibrillar angle varies from one plant fiber to another. The mechanical properties of the fiber are dependent on the cellulose content, microfibrillar angle and the degree of polymerization. Degree of polymerization also depends on the part of the plant from which fibers are obtained. Fibers with higher cellulose content, higher degree of polymerization and a lower microfibrillar angle exhibit higher tensile strength and modulus.

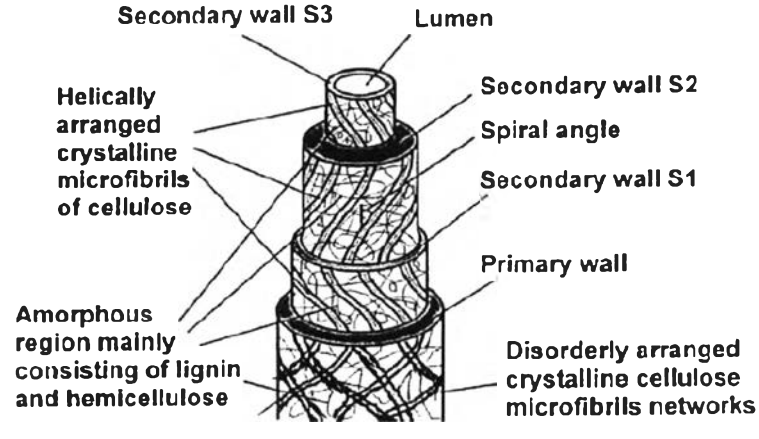

Figure 2.2 Structural constitution of natural vegetable fiber cell (Rong *et al.*, 2001).

2.2.3 Chemical Composition of Plant Fibers

The chemical composition as well as the morphological microstructure of vegetable fibers is extremely complex due to the hierarchical organization of the different compounds present at various compositions. Depending on the type of fiber, the chemical composition of natural fibers varies. Primarily, fibers contain cellulose, hemicellulose and lignin. The property of each constituent contributes to the overall properties of the fiber.

1. Cellulose

Cellulose forms the basic material of all plant fibers. It is generally accepted that cellulose is a linear condensation polymer consisting of D-anhydroglucopyranose units joined together by β-1 4-glycosidic linkages, as shown in Figure 2.3. Cellulose is thus a 1,4- β-Dglucan (Nevell and Zeronian, 1985).

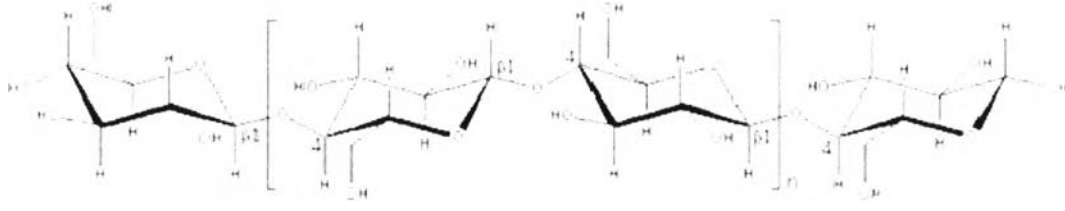

Figure 2.3 The structural unit of cellulose (Chaplin, 2009).

The molecular structure of cellulose, which is responsible for its supramolecular structure, determines many of its chemical and physical properties. In the fully extended molecule, the adjacent chain units are oriented by their mean planes at the angle of 180°C to each other. Thus, the repeating unit in cellulose is the anhydrocellobiose unit, and the number of repeating units per molecule is half the DP. This may be as high as 14,000 in native cellulose.

The mechanical properties of natural fibers depend on the cellulose type. Each type of cellulose has its own cell geometry, and the geometrical conditions determine the mechanical properties. Solid cellulose forms a microcrystalline structure with regions of high order, i.e., crystalline regions, and regions of low order, i.e., amorphous regions. Cellulose is also formed of slender rod like crystalline microfibrils. The crystal nature (monoclinic sphenodic) of naturally occurring cellulose is known as cellulose I. Cellulose is resistant to strong alkali (17.5 wt%) but is easily hydrolyzed by acid to water-soluble sugars. Cellulose is relatively resistant to oxidizing agents.

2. Hemicellulose

Hemicellulose is not a form of cellulose at all. It comprises a group of polysaccharides (excluding pectin) that remains associated with the cellulose after lignin has been removed. The hemicellulose differs from cellulose in three important

aspects (Nevell and Zeronian, 1985). In the first place, they contain several different sugar units, whereas cellulose contains only 1,4- β-D-glucopyranose units. Secondly, they exhibit a considerable degree of chain branching, whereas cellulose is strictly a linear polymer. Thirdly, the degree of polymerization of native cellulose is 10–100 times higher than that of hemicellulose. Unlike cellulose, the constituents of hemicellulose differ from plant to plant (Nevell and Zeronian, 1985; Frollini *et al.*, 2000).

3. Lignin

Lignins are complex hydrocarbon polymers with both aliphatic and aromatic constituents (Kalia *et al.*, 2011; Kritschewsky, 1985). Their chief monomer units are various ring-substituted phenyl propane linked together in ways that are still not fully understood. Their mechanical properties are lower than those of cellulose. Lignin is totally amorphous and hydrophobic in nature. It is the compound that gives rigidity to the plants. Lignin is considered to be a thermoplastic polymer, exhibiting a glass transition temperature of around 90°C and melting temperature of around 170°C. It is not hydrolyzed by acids, but soluble in hot alkali, readily oxidized and easily condensable with phenol (Sadov *et al.*, 1978).

4. Pectins and Waxes

Pectin is a collective name for heteropolysaccharides, which consist essentially of polygalacturon acid. Pectin is soluble in water only after a partial neutralization with alkali or ammonium hydroxide. It provides flexibility to plants. Waxes make up the last part of fibers and they consist of different types of alcohols, which are insoluble in water as well as in several acids.

2.2.4 Cellulose from Plant Fibers

A single fiber of all plant-based natural fibers consists of several cells. These cells are formed out of cellulose-based crystalline microfibrils, which are connected to a complete layer by amorphous lignin and hemicellulose. Multiples of such cellulose–lignin–hemicellulose layers in one primary and three secondary cell walls stick together to form a multiple layer composite. The fiber strength increases with increasing cellulose content and decreasing spiral angle with respect to fiber axis.

Cellulose is found not to be uniformly crystalline. However, the ordered regions are extensively distributed throughout the material, and these regions are called crystallites. The threadlike entity, which arises from the linear association of these components, is called the microfibril. It forms the basic structural unit of the plant cell wall. These microfibrils are found to be 10–30 nm wide, less than this in width, indefinitely long containing 2–30,000 cellulose molecules in cross section. Their structure consists of predominantly crystalline cellulose core. Individual cellulose nanocrystals (Figure 2.4) are produced by breaking down the cellulose fibers and isolating the crystalline regions (Oke, 2010). These are covered with a sheath of paracrystalline polyglucosan material surrounded by hemicelluloses (Whistler and Richards, 1970).

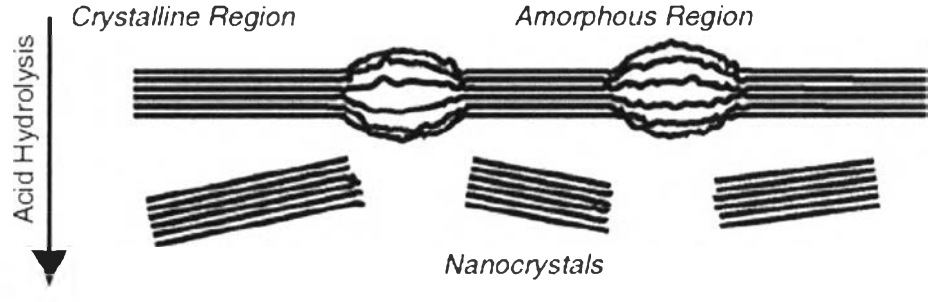

Figure 2.4 Acid hydrolysis breaks down disordered (amorphous) regions and isolates nanocrystals (Oke, 2010).

In most natural fibers, these microfibrils orient themselves at an angle to the fiber axis called the microfibril angle. The ultimate mechanical properties of natural fibers are found to be dependent on the microfibrillar angle. Gassan *et al.*, 2001) have done calculations on the elastic properties of natural fibers. Cellulose exists in the plant cell wall in the form of thin threads with an indefinite length. Such threads are cellulose microfibrils, playing an important role in the chemical, physical and mechanical properties of plant fibers and wood. Microscopists' and crystallographers' studies have shown the green algae Valonia to be excellent material for the ultrastructural study of the cellulose microfibril (David *et al.*, 1991). A discrepancy in the size of the crystalline regions of cellulose, obtained by X-ray diffractometry and electron microscopy, led to differing concepts on the molecular

organization of micro-fibrils. David *et al.* regarded the microfibril itself as being made up of a number of crystallites, each of which was separated by a para-crystalline region and later termed "elementary fibril" (Frey-Wyssling, 1954). The term "elementary fibril" is therefore applied to the smallest cellulosic strand. Electron micrograph studies of the disintegrated microfibrils show the crystalline nature of cellulose microfibrils (Magnfn 100 nm) taken by diffraction contrast in the bright field mode. Reports on the characterization and the make-up of the elementary fibrils and on their association while establishing the fiber structure – usually called fibrillar or fringed fibril structure are there in the literature (Krassig, 1992). According to this concept, the elementary fibril is formed by the association of many cellulose molecules, which are linked together in repeating lengths along their chains. In this way, a strand of elementary crystallites is held together by parts of the long molecules reaching from one crystallite to the next, through less ordered inter-linking regions. Molecular transition from one crystallite strand to an adjacent one is possible, in principle. Apparently, in natural fibers, this occurs only to a minor extent, whereas in man-made cellulosic fibers, such molecular transitions occur more frequently.

The internal cohesion within the elementary fibrils is established by the transition of the long cellulose chain molecules from crystallite to crystallite. The coherence of the fibrils in their secondary aggregation is given either by hydrogen bonds at close contact points or by diverging molecules. Access into this structure is given by large voids formed by the imperfect axial orientation of the fibrillar aggregates, interspaces of nanometre dimensions between the fibrils in the fibrillar aggregations and by the less ordered inter-linking regions between the crystallites within the elementary fibrils. Dufresne has reported on whiskers obtained from a variety of natural and living sources (Dufresne, 1998). Cellulose microfibrils and cellulose whisker suspension were obtained from sugar beet root and from tunicin. Typical electron micrographs obtained from dilute suspensions of sugar beet are shown in Figure 2.5. Individual microfibrils are almost 5 nm in width while their length is of a much higher value, leading to a practically infinite aspect ratio of this filler. They can be used as a reinforcing phase in a polymer matrix.

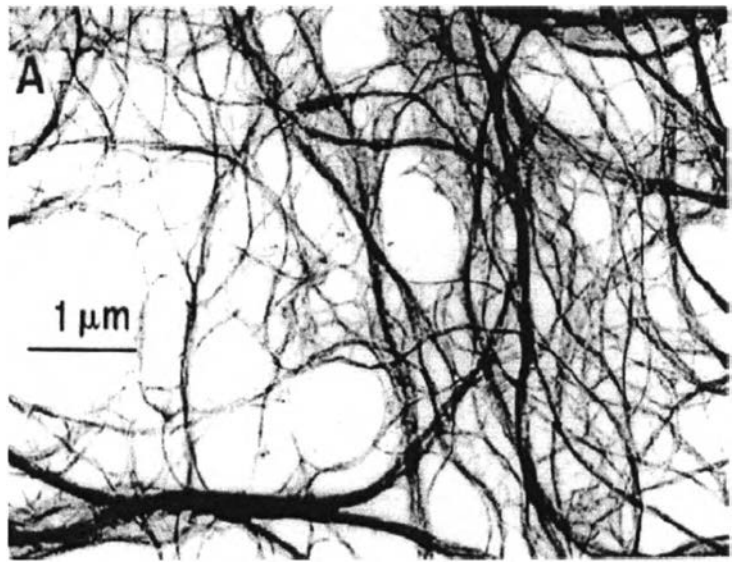

Figure 2.5 Transmission electron micrograph of a dilute suspension of sugar beet cellulose (Dufresne, 1998).

2.3 Natural Rubber

Natural rubber (NR), cis-1,4-polyisoprene (Figure. 2.6), is naturally produced by the Hevea brasiliensis trees which accounts for over 99% of the world's natural rubber production (Sakdapipanich *et al.*, 2007). Natural rubber latex is composed of about 36% of rubber, 5% of non-rubbers components (proteins, lipids, sugars, and ash) and water accounting for the remaining 59% (Sansatsadeekul *et al.*, 2011). Thailand can be considered as one of the most significant resource of NR (Wang *et al.*, 2009) so, NR is a low cost, available and renewable natural resource. The outstanding physical properties of NR are flexibility, high strength, good crack growth resistance and good processability and water resistance. It is currently used in more than 50 thousands in different products such as tire, adhesives, coating and floor covering (Ripel *et al.*, 2009).

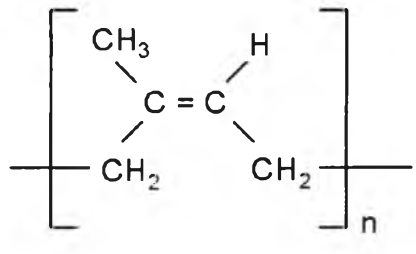

Figure 2.6 Chemical structure of cis-1,4-polyisoprene.

2.4 Plasma

2.4.1 Basic Principle of Plasma

Plasma is ionized gas. It consists of positive and negative ions, electrons, as well as free radicals. The ionization degree can vary from 100% (fully ionized gas) to very low values (partially ionized gas). The plasma state is often referred to as the fourth state of matter: solid, liquid, gas, and plasma (Lieberman and Lichtenberg, 2005). It is a collection of free charged particles moving in random directions that is, on the average, electrically neutral ($n_e \approx n_i$) (see Figure 2.7 a).

Plasma can occur in natural. Lightning and Auroras Borealis are the most common natural plasma observed on Earth (Fridman and Kennedy, 2004). However, plasmas can be generated artificially at laboratory levels for practical applications. It is understood that a continuous source of energy is required to generate and sustain a state of matter. Man–made plasmas are commonly generated and sustained using electrical energy and are often referred to as 'discharges'. A simple discharge is shown schematically in Figure 2.7 b. It consists of a voltage source that drives current through a low-pressure gas between two parallel conducting plates or electrodes. The gas "breaks down" to form a plasma, usually weakly ionized which is the plasma density only a small fraction of the neutral gas density (Lieberman and Lichtenberg, 2005).

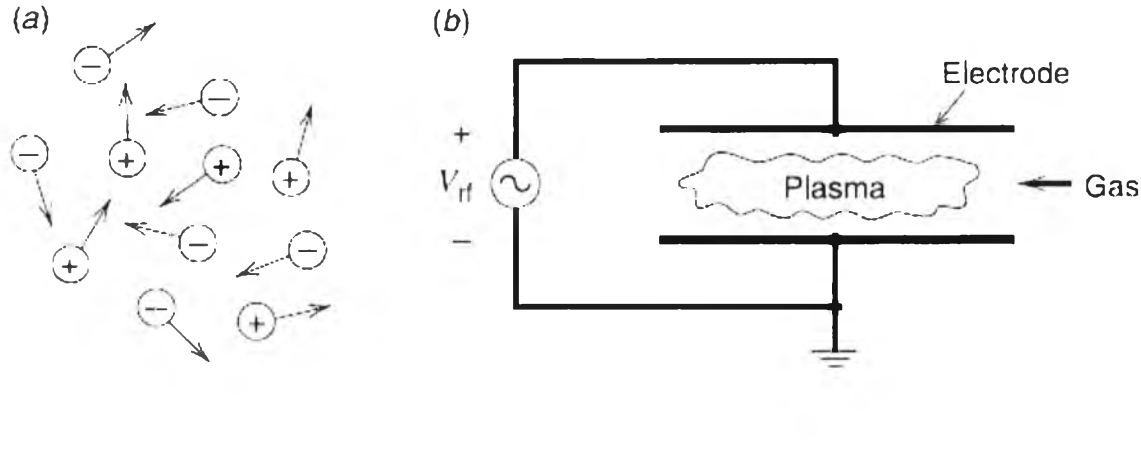

Figure 2.7 Schematic views of (a) a plasma and (b) a discharge.

There are four steps of plasma forming (Lieberman, and Lichtenberg, 2005).

1.) Solid state. At very low temperatures, matter is in a solid state with the atoms arranged in well-organized grids.

2.) Liquid state. When temperature increases above a critical value, solids melt and become a liquid. The grid of atom is broken, but molecular bonds are maintained.

3.) Gas state. A liquid heated above a second critical temperature turns into a gas. The molecules in the gas decompose to form a gas of atoms that move freely in random directions

4.) Plasma state. If the temperature is further increased, then the atoms decompose into freely moving charged particles (electrons and positive ions), and the substance enters the plasma state.

In general, plasmas are realized by the generation of free electrons that make the gas conductive. These electrons obtain energy from the electric field and further ionize, excite, and dissociate gas molecules via energy transfer during collisions. This makes plasmas very reactive. Also, plasmas possess higher temperatures and energy densities in comparison with most other chemical processes, which make them interesting and efficient for various applications. They can be generated over a wide range of pressures with different electron temperatures and densities. Most applied plasmas have electron temperatures between 1 – 20 eV (1 eV

$\approx$ 1.6 x 10^{-19} Joule $\approx$ 11600 K) and densities between 106 – 1018 (electrons/cm^3) (Fridman and Kennedy, 2004).

2.4.2 Classification of plasma

Plasma states can be divided in two main categories: thermal plasmas (equilibrium plasmas) and non-thermal plasma or cold plasma (non-equilibrium plasmas).

2.4.2.1 Thermal plasma or equilibrium plasma

As the name suggested, thermal plasmas are 'hot'. They have high gas temperatures (usually > 10,000 K). Thermal plasmas, an essential condition for the formation of this plasma is sufficiently high working pressure and low electric fields. In this type, the electron temperature (T_e) is approximately equal to neutral temperature (T_n), ($T_e \approx T_n$). These plasmas are usually sustained at high power densities (power input per unit volume) and have low chemical selectivity. The main drawbacks of using thermal plasmas for plasma chemical applications are the overheating of reaction media when energy is uniformly consumed by the reagents into all degree of freedom and, thus ,high energy consumption required to provide special quenching of the reagents. Etc. They are obviously of no interest to textile manufacturers (Fridman and kennedy, 2004). Lightning and thermal arc discharges are examples of naturally occurring and artificially generated thermal plasmas, respectively.

2.4.2.2 Non-thermal plasma or non-equilibrium plasma

While non-thermal plasma include low-pressure direct current (DC) and radio frequency (RF) discharges (silent discharges), and discharge from fluorescent (neon) illuminating tubes. Thermal condition of electron temperatures (T_e) is extremely higher than neutral temperatures (T_n), ($T_e > T_n$). The free electrons are very hot indeed, with typical temperatures ranging from 10,000 to 50,000 K, but the rest of the system, the ions and neutrals, is at or near room temperature. Because the free electrons comprise much, much less than one millionth of the total mass of the system, they have negligible heat capacity so that the actual heat content of the plasma is low. However, those hot, high energy electrons are keys to the power of plasma in its ability to change surfaces. They career madly around the plasma volume, colliding with the other microscopic components and generating a wealth of

new microscopic species with chemical and physical energy. They operate at low power densities, but have very good chemical selectivity. This plasma can be classified into several types depending upon their generation mechanism, their pressure range, and the electrode geometry. An example of non-thermal plasma is grow discharges, the operating pressures are normally less than 1 kPa and have electron temperatures of the order of 10^4 k with ions and neutral temperatures approaching room temperature (Fridman and kennedy, 2004; Shishoo, 2007). And other types of this plasma are auroras, radio frequency discharge, microwave discharge, corona discharge, and dielectric-barrier discharge (DBD), which the latter is used in this study.

2.4.3 Type of non-thermal plasmas

It is customary to divide non-equilibrium plasmas into distinctive groups, depending on the mechanism used for their generation, their pressure range, or the electrode geometry. In this section, the most notable characteristics of the following six non–thermal discharges are listed:

2.4.3.1 Glow discharge

The glow discharge is stationary and low-pressure discharge, usually generated between flat electrodes. The glow can be produced by applying a potential difference between electrodes in a gas. According to a more descriptive physical definition: a glow discharge is the self-sustained continuous DC discharge having a cold cathode, which emits electrons as a result of secondary emission mostly induced by positive ions. A schematic drawing of a typical normal glow discharge is shown in Figure 2.8. An importance distinctive feature of the general structure of a glow discharge is large positive space charge and strong electric field with a potential drop of about 100 to 500. The thickness of the cathode layer is inversely proportional to gas density and pressure. If the distance between electrodes is sufficiently large, Quasi-neutral plasma with a low electric field, the so-called positive column, is formed between the cathode layer and anode. The positive of a glow discharge is the most traditional example of weakly ionized, non-equilibrium, low-pressure plasma (Fridman and Kennedy, 2004).

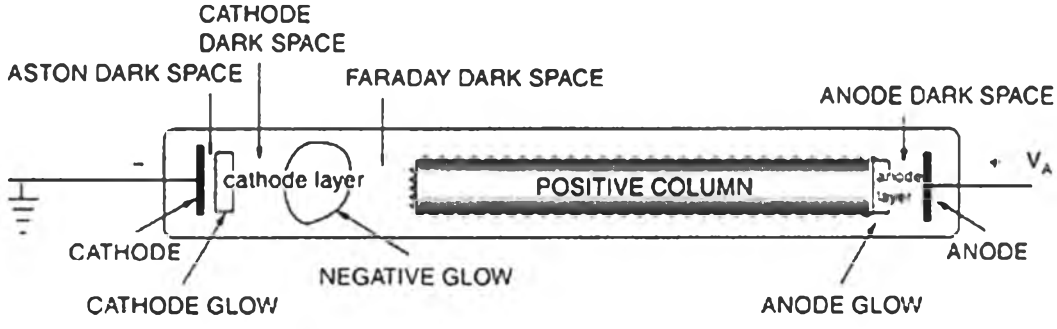

Figure 2.8 General structure of a glow discharge (Fridman and Kennedy, 2004).

One reason for the popularity of glow discharges is the comparatively low voltage and current needed to run them. It has become an important laboratory tool for plasma chemical investigation. In the lighting industry, the neon tubes used for outdoor advertising and the fluorescent tubes are examples of practical applications of glow discharges. However, the too low pressure and the resulting low mass flow, the glow discharge has not been used for industrial production of chemicals.

2.4.3.2 Radio Frequency discharge

The radio frequency (RF) discharges are used extensively in the laboratory to produce plasmas for optical emission spectroscopy and for plasma chemical investigation. RF discharges can be classified into two types according to the method of coupling the RF power with the load: capacitive coupling and inductive coupling. Figure 2.9 shows the setup typically consists of an RF generator, a matching network, and an antenna of capacitive coupling (Chu and Liu, 2008). RF discharges work well at low pressure, but are used also at atmospheric pressure. Low-pressure RF discharges for etching purposes have found widespread applications in semiconductor manufacturing. As long as the collision frequency is higher than the frequency of the applied field, the discharge behaves very much like a dc discharge. This implies that non-equilibrium conditions can be expected at low pressures, whereas thermal plasmas are generated at about atmospheric pressure.

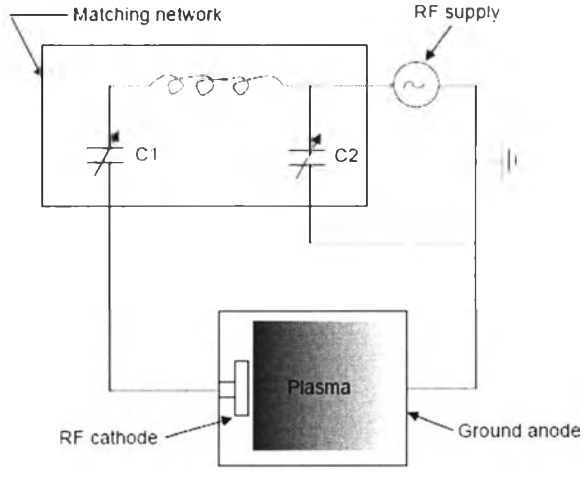

Figure 2.9 Schematic diagram of a capacitively-coupled plasma (CCP) plasma source with an equivalent electrical circuit.

2.4.3.3 Microwave discharge

The plasma is contained in a dielectric tube of a few centimeters diameter and is sustained by an electromagnetic wave, which uses only the plasma column and the tube as its propagating media. They can operate over a large frequency and pressure range and can produce large-volume non-equilibrium plasmas of reasonable homogeneity. Plasma columns of up to 4-m length have been thus produced. Due to the large pressure range, under which these discharges can be operated, electron densities between 10^{8} and 10^{15} cm^{-3} have been reported. Applications so far have been limited to elemental analysis and lasing media. The ease of operation and the possibility of imposing a gas flow make these discharges attractive also for plasma chemical investigations. An example of Microwave discharge as shown in Figure 2.10.

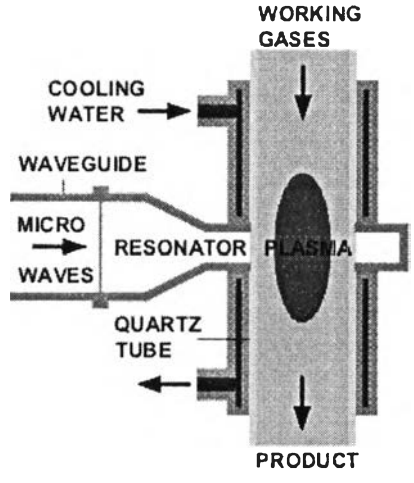

Figure 2.10 Schematic drawing of Microwave discharge.
(http://www.plasma.inpe.br/LAP_Portal/LAP_Site/Figures, 17 April 2009)

2.4.3.4 Gliding arc discharge

The gliding arc discharge is a non-thermal plasma technique, which has least two diverging knife-shape electrode. These electrodes are immersed in a fast flow of feed gas. A high voltage and relatively low current discharge are generated across the fast gas flow between the electrodes (Fridman and Kennedy, 2004). During the gliding arc evolution the plasma goes through a variety of different states and these phases of the gliding arc are shown in Figure 2.11.

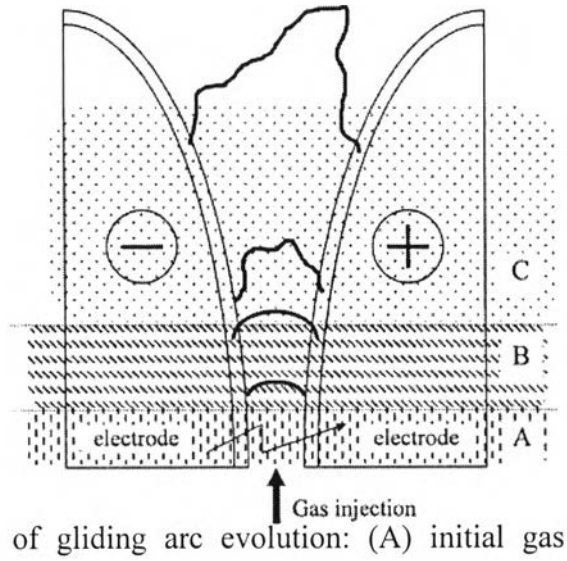

Figure 2.11 Phases of gliding arc evolution: (A) initial gas break-down; (B) equilibrium heating phase; (C) non-equilibrium reaction phase.

The initial break-down (A) of the processed gas begins the cycle of the gliding arc evolution. The high voltage generator provides the necessary electric field to break down the air between the electrodes and the discharge starts at the shortest distance (1–2 mm) between the two electrodes (Fridman and Kennedy, 2004).

The equilibrium stage (B) takes place after formation of a stable plasma channel. The gas flow at a velocity of about 10 m/s and the length of the arc column increase together with voltage (Fridman and Kennedy, 2004).

The non-equilibrium stage (C) When the length of the gliding arc exceeds its critical value, heat losses from the plasma column begin to exceed the energy supplied by the source, so it is not possible to sustain the plasma in the state of thermodynamic equilibrium. As a result, the discharge plasma rapidly cools to the gas temperature (about T_0 = 2000 K) while the plasma conductivity is maintained by a high value of the electron temperature Te = 1 eV (about 11,000 K). After the decay of the non-equilibrium discharge, there is new breakdown at the shortest distance between electrodes and the cycle repeats (Fridman and Kennedy, 2004).

2.4.3.5 Corona discharge

Corona discharges are plasmas that result from the high electric field that surrounds an electrically conductive spatial singularity when a voltage is applied. Corona generation systems usually take the form of two opposing electrically conductive electrodes separated by a gap containing the gas from which the plasma is generated and connected to a high voltage source. Corona discharge differs from glow discharge (weak current) and arc discharge (high current) with respect to the flow of current. The high electric field around the singularity, i.e. the point of the needle or the wire, causes electrical breakdown and ionisation of whatever gas surrounds the singularity, and plasma is created, which discharges in a fountain-like spray out from the point or wire (Shishoo, 2007). One way of stabilizing the discharge at high pressure is the use of inhomogeneous electrode geometries, e.g. a point electrode and a plane, such as in Figure 2.12, or a thin wire.

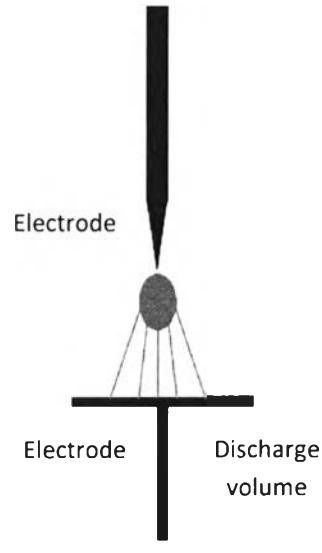

Figure 2.12 The corona discharge-inhomogeneous discharge at atmospheric pressure.

2.4.3.6 Dielectric barrier discharge

A dielectric barrier discharge (DBD) is generated in the space between two electrodes, each of which is covered with an insulating, dielectric coating. Sometimes dielectric-barrier discharges are also called silent discharges because of the absence of sparks that are accompanied by local overheating, generation of local shock waves, and noise (Fridman and Kennedy, 2004). A DC, AC, or pulsed high voltage is applied to the electrodes, which stimulates electron emission from the instantaneous cathode. These electrons avalanche to form a filament across the gap. DBD plasma has inherent advantages over the discharges, which have been treated until now. It combines the large volume excitation of the glow discharge with the high pressure of the corona discharge. The main elements of dielectric barrier discharge configuration are shown in figure 2.13.

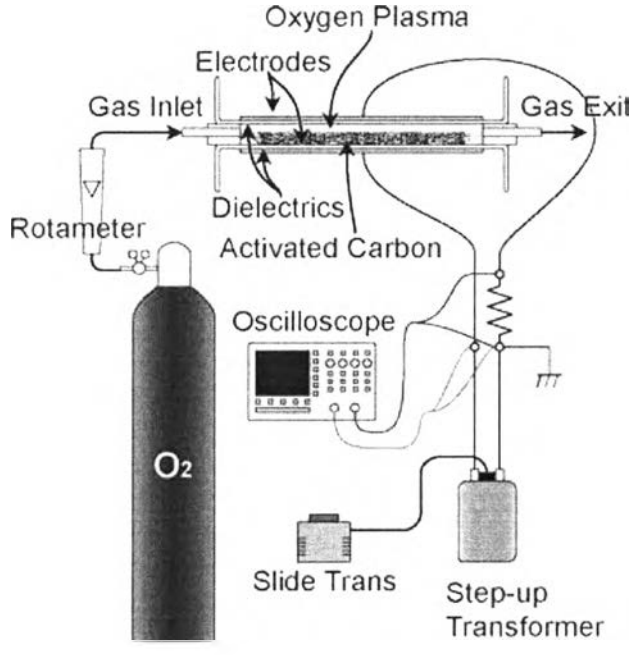

Figure 2.13 Experimental set up of dielectric barrier discharge plasma (DBD) (Agostino *et al.*, 2005).

DBD plasmas are normally operated in one of the parallel-plate (Figure 2.14) or cylindrical (Figure 2.15) configurations. The parallel-plate configuration is used to surface treat fast-moving webs and films, and the annular volume of the cylindrical configuration is used to treat airflows for ozone production. At least one electrode of these geometries is covered with an insulating dielectric barrier to prevent real currents from flowing from the discharge volume to the electrodes and power supply.

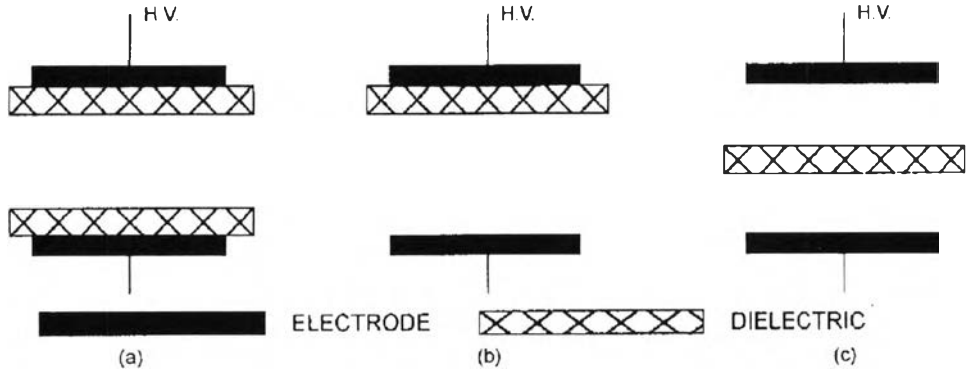

Figure 2.14 Schematic diagram of parallel-plate DBD plasma source configurations.

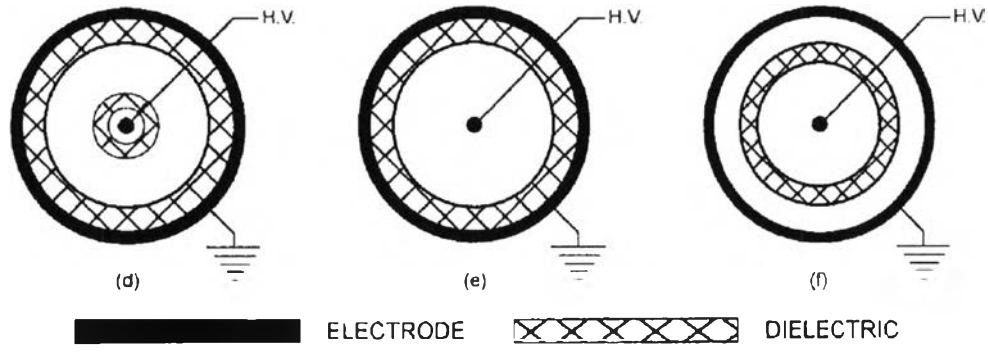

Figure 2.15 Schematic diagrams of cylindrical DBD plasma source configurations.

2.4.4 Interaction of Plasmas with Polymer Surfaces

In the plasma treatment of polymers, energetic particles and photons generated in the plasma interact strongly with the polymer surface, usually via free radical chemistry. In plasma which does not give rise to thin film deposition, four major effects on surfaces are normally observed. Each is always present to some degree, but one may be favored over the others, depending on the substrate and the gas chemistry, the reactor design, and the operating parameters. The four major effects are:

1.) Surface cleaning, that is, removal of organic contamination that interferes with adhesion processes.

2.) Ablation or etching of material from the surface, it is important for cleaning of badly contaminated surface, for the removal of weak boundary and increase the surface area.

3.) Cross-linking of near-surface molecules, which can cohesively strengthen the surface layer.

4.) Modification of surface-chemical structure, which can occur during plasma treatment itself, and upon re-exposure of the treated part to air, at which time residual free radicals can react with atmospheric oxygen or water vapor.

Plasma treatment can be used with great effect to improve the bond strength of polymer to fiber and polymer to polymer combinations. In these cases, the improved adhesion results from both increased wettability of the treated substrate and the modification of surface chemistry of the polymer (Mittal, 2000).

Carla *et al.* (2009) treated additive-free hand sheet paper samples with cold plasma and grafted reactive natural products, namely myrcene (My) and limonene (LM) on the cellulose. Argon was used as the carrier gas. Three different processing conditions were tested. The first one was based on the activation of the paper surface by plasma discharge followed by its immersion into the monomeric liquid. The second approach called on the impregnation of the substrate to be treated by the chosen monomer and then the exposure of the impregnated sheet to plasma discharge. Finally, the third method was based on impregnation of the paper sample followed by its plasma activation and then again its immersion into the monomeric liquid. After the grafting, they found that the contact-angle value of a drop of water deposited at the surface of paper increased. . The treated surfaces displayed water-barrier properties; the penetration of the liquid was reduced significantly after LM and My treatments. The XPS spectra showed that the modification with LM and My can make the O/C of the grafted decreases.

In 2011, Zhou *et al.* improved ramie fiber surface properties for better adhesion to polypropylene by using atmospheric pressure plasma jet (APPJ) treatment with ethanol pretreatment. They soaked ramie fiber in ethanol for 10 min and treated it with helium plasma. Scanning electron microscopy shows increased the plasma treated fiber surface roughness due to plasma etching and X-ray photoelectron spectroscopy analysis indicates increased carbon contents and hydrophobic C–C bonds. IFSS values between ramie and PP fibers were increased by nearly 50% due to the creation of a more hydrophobic surface of ramie fibers by the reaction of ethanol molecules to cellulose in plasma treatment and the roughened fiber surface that enhanced mechanical keying between the fiber surface and the matrix. So, the employment of ethanol pretreatment and plasma treatment can effectively induce hydrophobic surface modification of cellulose fiber to enhance the compatibility to polypropylene (PP) matrix.

Calvimontes *et al.* (2011) studied the effects of the exposure of Cellophane foils to low-pressure oxygen plasma on topography, chemical composition and morphology. They found that the plasma exposure resulted in physical and chemical changes on cellulose surfaces. According to the XPS measurements (Figure 2.16), plasma reactions changed the surface chemistry by

decomposition of polymer chains and oxidation reactions forming aldehyde and carboxylic acid/carboxylate groups. From XRD, it indicated that the crystalline domains are not influenced by plasma treatments.

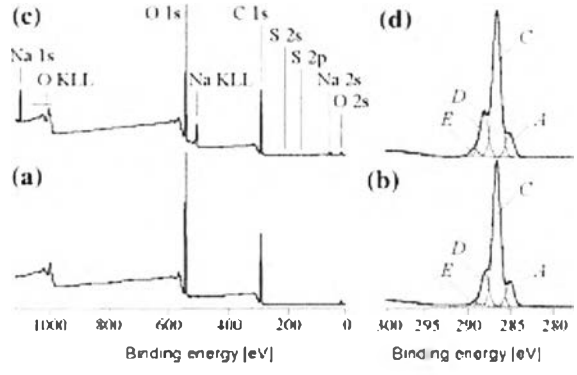

Figure 2.16 Wide-scan (a,c) and C 1 s high-resolution (b,d) spectra of an untreated (a, b) Cellophane foil sample and a sample, which was treated in an oxygen plasma for 480 s (c, d).

In 2012, hydrophobic finishing of cellulosic substrate was investigated by using He/1,3-butadiene plasma at atmospheric pressure. As shown in Table 2.1, after plasma treatment, water absorbency time in the 12 min plasma treated sample increased from <1 s to >60 min and contact angle from ~0° to 142° compared to the untreated sample. Moreover, SEM images showed a thin polymer layer on sample surface after plasma. The result shows that the He/BD plasma was successfully utilized to impart a high degree of hydrophobic functionality to cellulosic fabric (Samanta *et al.*, 2012).

Table 2.1 Water droplet absorbency time and contact angle in the untreated and He/BD plasma treated cellulosic samples

Plasma treatment conditions	Water absorbency time		Contact angle (°)	
	As-prepared sample	Soap washed sample	As-prepared sample	Soap washed sample
Untreated sample	<1 s	<1 s	~0°	~0°
He 2500 ml/min; BD 500 ml/min; treatment time: 1.5 min	28.5 min	14 s	<90°; not measureable	<90°; not measureable
He 2500 ml/min; BD 500 ml/min; treatment time: 7 min	≫60 min	103 s	143°	130°
He 2500 ml/min; BD 500 ml/min; treatment time: 12 min	≫60 min	250 s	142°	134°
He 500 ml/min, BD 10 ml/min; treatment time: 12 min	≫60 min	41.5 min	138°	117°
He 500 ml/min, BD 40 ml/min; treatment time: 12 min	≫60 min	≫60 min	143°	128°

2.5 ZnO Particles

2.5.1 Basic Properties and Applications

ZnO has been widely studied since 1935 and its unique properties have been intensively reviewed. ZnO is a metal oxide, and the Zn-O is bonded with a very strong ionic character (Jagadish *et al.*, 2006). Furthermore, it has gained more attention in many applications, such as food packaging, catalysis, sensors, environmental remediation, medicine, and personal care (Tayel *et al.*, 2010; Raghupathi *et al.*, 2011), because it is believed to be nontoxic, biological safety, and biocompatible. In packaging applications, ZnO provides several advantages, such as oxygen barrier property and antibacterial activity. It also acts as a crosslinking agent as well as a filler to enhance the mechanical property (Przybyszewska *et al.*, 2009; Zhao and Li, 2006).

ZnO has wide band gap energy equal to 3.36 eV, which absorbs the UV-light at below 380 nm (Padmavathy *et al.*, 2008). There are two crystallinity forms of ZnO: wurtzite and zincblend. (Figure 2.17) The wurtzite structure is a kind of hexagonal unit cell which the lattice parameters of a equal to 3.2495 Å and c equal to 5.2069 Å while the zincblend structure is a cubic unit cell which the lattice parameters of a equal to b equal to c (Jagadish *et al.*, 2006).

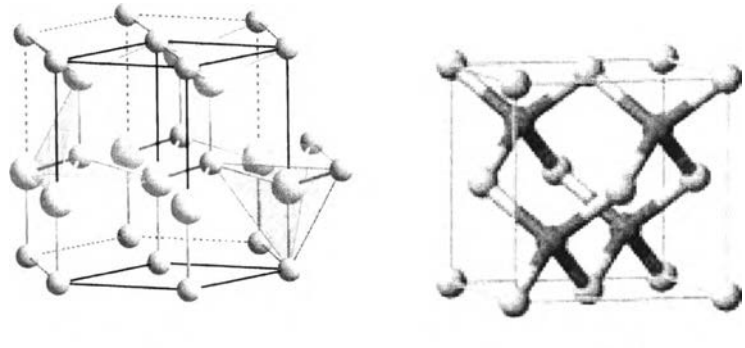

Figure 2.17 Wurtzite (a) and zincblend phases (b) of ZnO (Jagadish *et al.*, 2006).

2.5.2 ZnO Syntheses

There are many methods to synthesize ZnO, such as alkaline precipitation, organic-zinc hydrolysis, and spray pyrolysis. The different synthesis methods and conditions yield ZnO with different morphologies.

2.5.2.1 Alkaline Precipitation

This procedure is used to synthesize ZnO at room temperature by mixing zinc nitrate ($Zn(NO_3)_2$) or zinc acetate ($Zn(CH_3COO)_2$) with alkaline solutions, such as ammonium hydroxide (NH_4OH), sodium hydroxide (NaOH), and potassium hydroxide (KOH). After a drop-wise addition of alkaline solutions, the white particles of ZnO are obtained.

2.5.2.2 Organo-Zinc Hydrolysis

The organo-zinc, such as zinc t-butoxide, is used as a precursor by mixing t-butanol with diethylzinc hexane solution, thus yielding the ZnO particles.

2.5.2.3 Spray Pyrolysis

This procedure is used to synthesize the ZnO particles at high temperatures (Li and Haneda, 2003).

2.5.3 ZnO Crosslinking

Zinc oxide is a very effective ionic promoter agent and yields vulcanizates with one of the highest tensile strength. The crosslinking occurs via the reaction of carboxylic groups with zinc oxide, resulting in the formation of carboxylic salts, considered to be ionic crosslinks as shown in Figure 2.18. In contrast to the covalent crosslinks, ionic crosslinks are multifunctional and labile. Carboxylic salts group together, forming clusters or multiplets (Przybyszewska *et al.*, 2009).

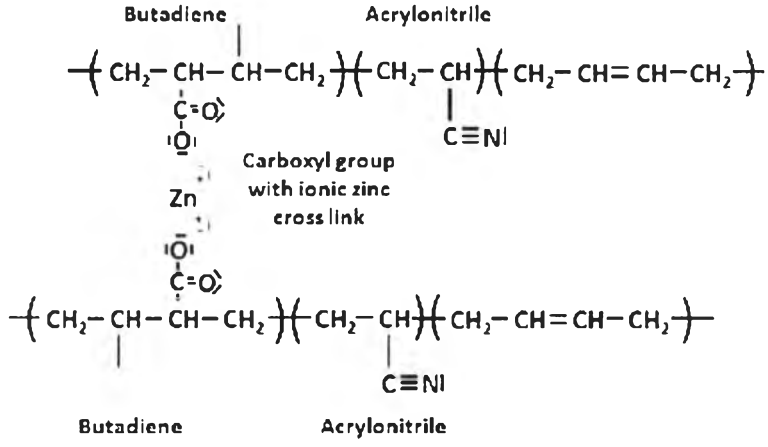

Figure 2.18 The crosslinking of carboxylated nitrile rubber with zinc oxide.

Antony *et al.* (2000) developed an ionic thermoplastic elastomer from ionomeric polyblends based on zinc salts of carboxylated nitrile rubber and poly(ethylene-co-acrylic acid. The ionomeric polyblends show higher physical properties than the corresponding non-ionomeric polyblends.

Przybyszewska *et al.* (2009) studied the activity of several nanosized zinc oxides in the crosslinking of carboxylated nitrile elastomer (XNBR). The results showed that the application of zinc oxide nanoparticles allowed for the realisation of vulcan-isates with considerably better mechanical properties and higher crosslink density, as compared to vulcanisates crosslinked with microsized zinc oxide.